Fabrication of low loss dispersion engineered chalcogenide photonic crystals

Marcel Spurny,[1,*] Liam O'Faolain,[1] Douglas A. P. Bulla,[2] Barry Luther-Davies,[2] and Thomas F. Krauss[1]

[1]*School of Physics & Astronomy, University of St. Andrews, St. Andrews, Fife KY16 9SS, UK*
[2]*ARC Centre for Ultrahigh bandwidth Devices for Optical Systems (CUDOS), Laser Physics Centre, Australian National University, Canberra ACT 0200, Australia*
**ms628@st-andrews.ac.uk*

Abstract: We demonstrate low loss photonic crystal waveguides in chalcogenide ($Ge_{33}As_{12}Se_{55}$) glasses. The measured losses are as low as 21dB/cm. We experimentally determine the refractive index of the thin film chalcogenide glass to be n = 2.6 and demonstrate that dispersion engineering can be performed up to a group index of n_g = 40 in this relatively low refractive index contrast system.

OCIS codes: (230.5298) Photonic crystals; (220.4000) Microstructure fabrication; (190.4360) Nonlinear optics, devices; (130.5296) Photonic crystal waveguides.

References and links

1. T. K. Liang, and H. K. Tsang, "Optical Limiting and Raman Amplification in Silicon Waveguides", in *Optical Fiber Communication Conference and Exposition and The National Fiber Optics Engineers Conference*, Technical Digest (CD) (Optical Society of America, 2005), paper JWA15.
2. M. Dinu, F. Quochi, and H. Garcia, "Third-order nonlinearities in silicon at telecom wavelengths," Appl. Phys. Lett. **82**(18), 2954–2956 (2003).
3. V. Mizrahi, K. W. Delong, G. I. Stegeman, M. A. Saifi, and M. J. Andrejco, "Two-photon absorption as a limitation to all-optical switching," Opt. Lett. **14**(20), 1140–1142 (1989).
4. D. Lezal, J. Pedlikova, and J. Zavadil, "Chalcogenide Glasses for optical and photonics applications," Chalcogenide Lett. **1**, 11–15 (2004).
5. K. A. Cerqua-Richardson, J. M. McKinley, B. Lawrence, S. Joshi, and A. Villeneuve, "Comparison of nonlinear optical properties of sulfide glasses in bulk and thin film form," Opt. Mater. **10**(2), 155–159 (1998).
6. Y. Ruan, M. Kim, Y. Lee, B. Luther-Davies, and A. Rode, "Fabrication of high-Q chalcogenide photonic crystal resonators by e-beam lithography," Appl. Phys. Lett. **90**(7), 071102 (2007).
7. K. Suzuki, Y. Hamachi, and T. Baba, "Fabrication and characterization of chalcogenide glass photonic crystal waveguides," Opt. Express **17**(25), 22393–22400 (2009).
8. S. A. Schulz, L. O'Faolain, D. M. Beggs, T. P. White, A. Melloni, and T. F. Krauss, "Dispersion engineered slow light in photonic crystals: a comparison," J. Opt. **12**(10), 104004 (2010).
9. M. Bass, ed., *Handbook of Optics II*, 2nd ed. (McGraw-Hill, 1994).
10. T. P. White, L. O'Faolain, J. Li, L. C. Andreani, and T. F. Krauss, "Silica-embedded silicon photonic crystal waveguides," Opt. Express **16**(21), 17076–17081 (2008).
11. J. Li, T. P. White, L. O'Faolain, A. Gomez-Iglesias, and T. F. Krauss, "Systematic design of flat band slow light in photonic crystal waveguides," Opt. Express **16**(9), 6227–6232 (2008).
12. A. Gomez-Iglesias, D. O'Brien, L. O'Faolain, A. Miller, and T. F. Krauss, "Direct measurement of the group index of photonic crystal waveguides via Fourier transform spectral interferometry," Appl. Phys. Lett. **90**(26), 261107 (2007).

Introduction

The increasing demand for bandwidth in telecommunication systems suggests that all-optical signal processing based on nonlinear effects will become essential in the long term. In silicon, the obvious material for photonic-electronic integration, nonlinear processes are limited by nonlinear loss mechanisms, such as two-photon absorption (TPA) and subsequent free carrier absorption (FCA) [1]. At the telecom wavelength of $\lambda = 1540nm$, the high TPA coefficient of $\beta_2 \approx 0.79cm/GW$ results in a nonlinear figure of merit of $FOM = n_2/\beta_2\lambda \approx 0.37$ despite the sizeable nonlinear refractive index of $n_2 \approx 0.45 \cdot 10^{-13} cm^2/W$ [2]. The nonlinear figure of merit is very useful for comparing the suitability of materials for all-optical signal processing [3] irrespective of the waveguide geometry employed. Chalcogenide glasses, for example, offer a

#137250 - $15.00 USD Received 3 Dec 2010; revised 13 Jan 2011; accepted 13 Jan 2011; published 19 Jan 2011

much higher nonlinear figure of merit of typically FOM>>1. These glasses contain one or more of the chalcogen elements (sulphur, selenium or tellurium) from group 16 of the periodic table as a major constituent combined with glass-forming elements such as As, Ge, Sb, Ga, etc. Being composed of covalently bonded heavy elements leads to a window of transparency ranging from the near- well into the middle infrared [4]. Their high nonlinear refractive index in the range of $n_2 \approx 1\text{-}30 \cdot 10^{-14} cm^2/W$ combined with a low two-photon absorption coefficient, typically $\beta_2 < 1 \cdot 10^{-11} cm/GW$, makes them ideal candidates for nonlinear optical applications [5]. Previous work on chalcogenide photonic crystals has focused on cavities [6] and more recently, nonlinear optical effects have also been demonstrated in chalcogenide photonic crystal waveguides [7] that used silver doping to increase n_2 (but also β). Clear evidence for the benefits of using photonic crystals in the slow light regime is still missing, however, and a key stepping stone towards this important demonstration is the development of dispersion-engineered slow light photonic crystal waveguides in highly nonlinear materials. Here, we report the successful fabrication of dispersion engineered chalcogenide waveguides in the slow light regime and demonstrate low loss operation, both of which are important stepping-stones towards efficient nonlinear operation.

Slow light is an important phenomenon for enhancing nonlinear operations, however, it has only been realized so far in high contrast silicon waveguides using various techniques [8]. It is not obvious that the same techniques can be applied to lower refractive index systems. We highlight the issue in Fig. 1, which displays the dispersion curves of the even mode of a photonic crystal W1 waveguide for materials with a refractive index of $n \approx 2.6$ (e.g. chalcogenide, dashed), and $n \approx 3.48$ (i.e. silicon, solid) with respect to the light line (straight dashed). It is clear that the useful k-space between the light line and the cut-off point for AMTIR-1 is much smaller than that for silicon. The corresponding wavelength ranges are $\Delta\lambda \approx 87nm$ for silicon and $\Delta\lambda \approx 28nm$ for chalcogenide, which clearly limits the performance of the chalcogenides. Firstly, the operation is closer to the band-edge, which can increase linear losses, and secondly, the window for dispersion engineering is much smaller. Despite these considerable limitations, we demonstrate here that dispersion engineering methods can indeed be applied very successfully.

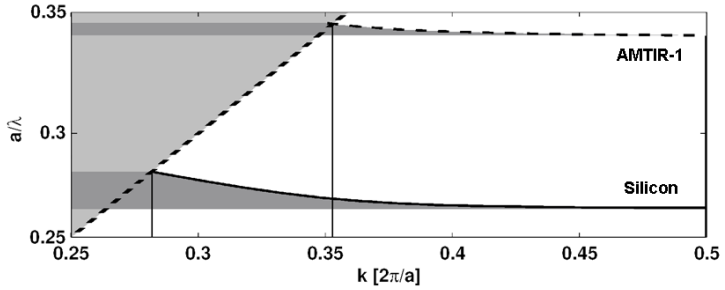

Fig. 1. Band diagram for the fundamental mode of a W1 photonic crystal waveguide for silicon (solid curve, n = 3.48) and AMTIR-1 ($Ge_{33}As_{12}Se_{55}$, n = 2.6, dashed curve). The light cone is outlined as the light grey area which is delimited with the straight dashed line. The dark grey areas outline the useful frequency range that is accessible below the light line and above the cut-off frequency. The corresponding accessible k-range lies between the crossing point of the dispersion curve of the respective material (denoted by the vertical solid lines) and the band edge at $k = \pi/a$. It is obvious that the operating range for the lower index contrast chalcogenide system is much smaller than that for the higher contrast silicon system.

Fabrication and loss measurements

Our devices were fabricated from a *300nm* layer of AMTIR-1 that had been deposited by thermal evaporation onto *1.5μm* of silica on a silicon substrate. The photonic crystal pattern was exposed in ZEON ZEP 520A electron-beam resist using a ZEISS GEMINI 1530/ RAITH ELPHY system. In order to achieve high resolution, an acceleration voltage of *30kV* was chosen with a write field size of *100μm* and pixel size of *2nm*. The electron beam resist was

#137250 - $15.00 USD Received 3 Dec 2010; revised 13 Jan 2011; accepted 13 Jan 2011; published 19 Jan 2011

developed using Xylene at *23℃* and the pattern was transferred into the chalcogenide layer using chemically assisted ion beam etching (CAIBE) with a chlorine/argon gas combination. The sample was heated to *T = 115℃* and a chlorine flow of 2.5sccm was used. For the argon beam, a flow rate of 2.5sccm was used with a beam current of 7.5mA and a beam voltage of 300V. These conditions required an etching time of 9 min and resulted in vertical sidewalls. The remaining electron beam resist was then removed by dimethylformamide. Due to the lower mechanical stability of AMTIR-1 compared to silicon, the use of liquid hydrofluoric (HF) acid to create the photonic crystal membrane had a very low success rate. Figure 2(a) shows a collapsed waveguide taper from the access waveguide to the photonic crystal waveguide. The stresses related to the liquid HF etching step tend to break away the mechanically sensitive taper from the photonic crystal membrane. To address this issue, we developed a vapour HF technique which avoids the disruptive surface tension. Hydrofluoric acid vapour reacts with silicon dioxide according to:

$$4HF + SiO_2 \rightarrow SiF_4(g) + 2H_2O. \quad (1)$$

The resulting water can condensate on the sample and react with the surrounding HF vapour to form liquid phase HF. In order to avoid such condensation, it is essential to keep the sample at elevated temperature. In fact, controlling the temperature gives a means of finely controlling the etch rate down to a few nm/minute. In order to implement the technique, we use a standard HDPE bottle that was partially filled with a 48% HF solution. The lid of the bottle incorporated a heater. The sample was then glued to the inside of the lid with standard heat sink paste in order to increase the thermal conductivity. The sample was heated up to *T = 50℃* in order to start the etch process. The temperature was then increased to *T = 70℃* over 3-4h. Controlling both, the temperature and the atmosphere gave fine control over the etch rate and time. Figure 2(b) shows the resulting successful application of HF vapour phase etching to chalcogenide photonic crystal waveguides. The access taper is partially suspended but clearly still connected to the photonic crystal waveguide, in contrast to the device shown in Fig. 2a that was etched using the liquid phase etching process.

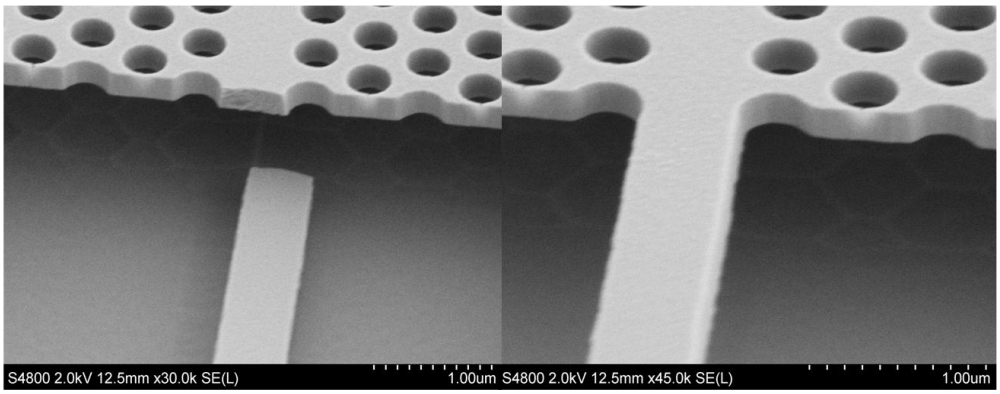

Fig. 2. Scanning electron micrographs of AMTIR-1 photonic crystal waveguides at the coupling section to the taper for the access waveguides. The smooth and vertical sidewalls of the holes are shown. (a) The access taper is collapsed due to stress acting on the waveguide and membrane during the liquid HF process. (b) An intact photonic crystal coupling section due to the use of vapour HF.

To avoid sagging of the under-etched access taper, a new design for the access waveguides was used. We widened the access waveguides from *3μm* to *6μm* and added a *50μm* long taper region. Figure 3(a) shows a sketch of this taper layout and Fig. 3(b) shows a corresponding cleaved facet. The remaining *2μm* wide silica under the waveguide acts as a supporting pedestal. The advantage of this new design is that no etch mask is required for the HF step,

#137250 - $15.00 USD Received 3 Dec 2010; revised 13 Jan 2011; accepted 13 Jan 2011; published 19 Jan 2011

thus reducing the number of processing steps and the exposure of the chemically sensitive chalcogenides to resist developer and remover.

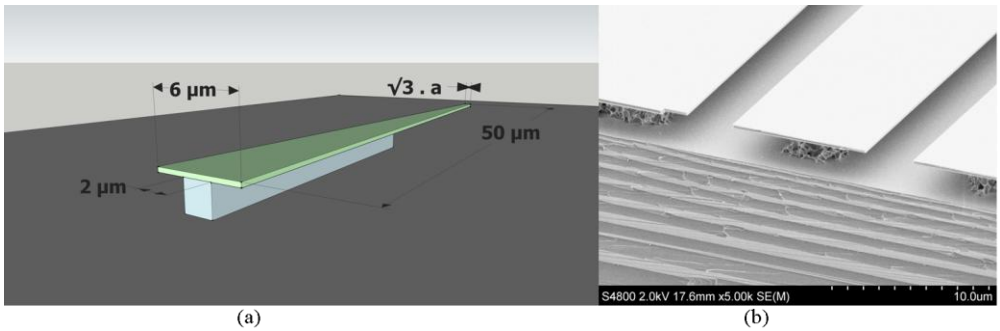

Fig. 3. (a) Sketch of the taper which allows performing the HF undercut without an additional masking step. The 6µm wide waveguide is tapered down to the waveguide width of 909nm within 50µm. The supporting, not-etched pedestal can be seen. (b) Cleaved facet of the access waveguide after underetching also showing the remaining silica which acts as a supporting pedestal under the access waveguide.

To determine the refractive index of the AMTIR-1 layer experimentally, we fabricated a set of *80µm* long photonic crystal waveguides with a range of lattice constants, whilst keeping the air hole fill-factor constant. The measured spectra were then matched to 3D MPB simulations, using the refractive index as a fitting parameter. The best match was achieved for a refractive index of $n = 2.6$ which agrees reasonably well with the literature bulk value of $n = 2.54$ [9]. We then fabricated W1s with a lattice constant of $a = 525nm$ and lengths varying from *95µm* to *1095µm* with a typical hole diameter of $d = 315nm$ ($r/a = 0.3$). The high quality of the fabrication process could be assessed from the sharpness of the transitions near cut-off as well as from cut-back measurements which determined the propagation loss (see Fig. 4). The transmission was found to drop by 35dB over a range of 3 nm near the band-edge suggesting our samples were of high quality (Fig. 4(a)). Cut-back measurements confirmed this and showed the loss, determined from plots of transmission versus length (Fig. 4(b)), was *21dB/cm*. Given the relative immaturity of chalcogenide photonic crystals, this compares well with losses of *12dB/cm* obtained for a silicon membrane W1 waveguide fabricated with the same lithography system [10].

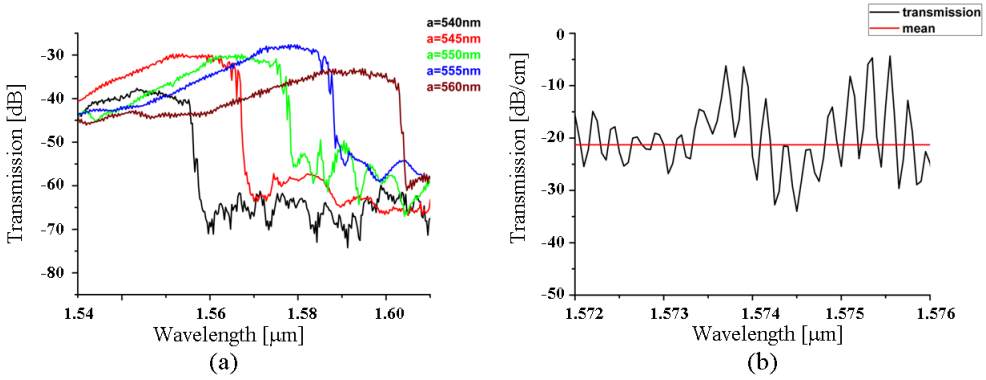

Fig. 4. a) Transmission measurements of the chalcogenide W1 photonic crystal waveguides for the determination of the refractive index. b) Losses extracted from cut-back measurements.

Dispersion engineering in low-index photonic crystal waveguides and experiments

We used the method based on shifting rows of holes to engineer the dispersion curve to produce a slow-light regime as was pioneered in silicon [11] using the group-index-

#137250 - $15.00 USD Received 3 Dec 2010; revised 13 Jan 2011; accepted 13 Jan 2011; published 19 Jan 2011

bandwidth-product (GIBP) $n_g(\Delta\omega/\omega)$ as a figure of merit (Fig. 5(a)). As expected for a lower refractive index material, the GIBP reaches a somewhat lower value of about 0.25, compared to 0.3 that can be achieved in silicon. Another difference is that the highest achievable group-index is around $n_g \approx 40$ rather than >100. Both of these observations highlight the reduced degrees of freedom given by the lower refractive index contrast, which also agrees with the smaller operating window observed in Fig. 1.

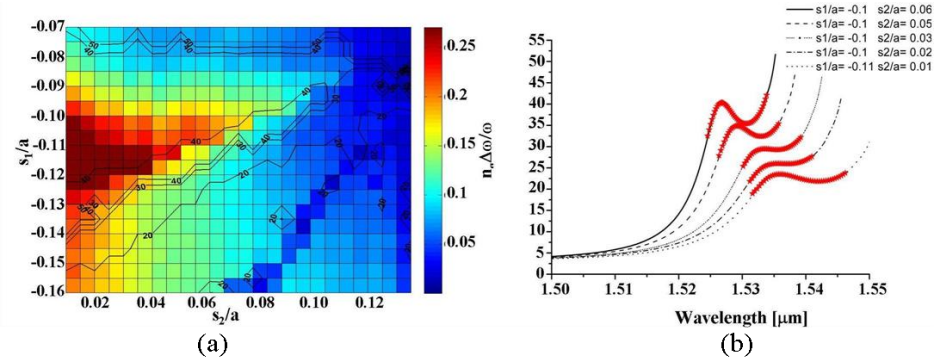

Fig. 5. (a) Map of 3D calculations for the group-index-bandwidth-product (as a function of s1 and s2). The color map displays the calculated GIBP whilst the contours map the achievable group index. (b) Calculated group index curves for modified W1 modes for certain values for s1 and s2. The red areas indicate the constant ($n_g \pm 10\%$) group index regions.

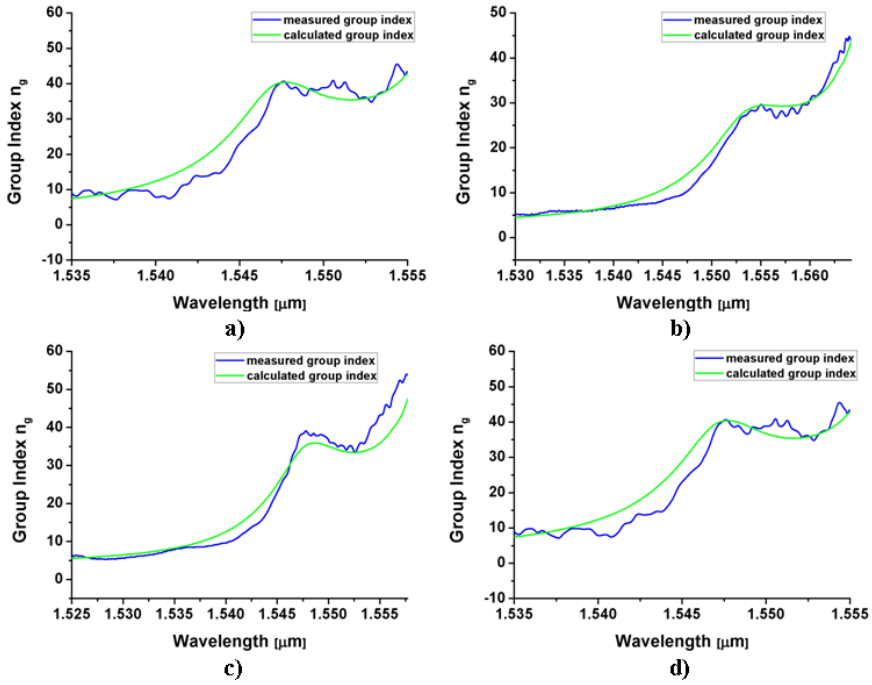

Fig. 6. Measured group indices (blue) and calculated group indices (green) for different lattice shifts. (a) s1/a = –0.1 s2/a = 0.02, (b) s1/a = –0.1 s2/a = 0.03, (c) s1/a = –0.1 s2/a = 0.05, (d) s1/a = –0.1 s2/a = 0.06.

The GIBP map was used to confirm the experimental design and Fig. 5(b) shows the group-index curves including the four different designs that were used for the fabrication of chalcogenide slow light samples. Figure 6 shows the measured group-index curves for four

#137250 - $15.00 USD Received 3 Dec 2010; revised 13 Jan 2011; accepted 13 Jan 2011; published 19 Jan 2011

different designs with a target n_g of 20, 30, 35 and 40. The measurements were carried out using Fourier transform spectral interferometry [12]. It is clear that despite the lower refractive index contrast, sizeable group index values can be achieved, e.g. $n_g \approx 40$ over a 5 nm bandwidth (Fig. 6d), thus highlighting the suitability of the method.

Conclusion

Chalcogenide photonic crystals are a favorable platform for nonlinear optics due to their high nonlinear figure of merit. Due to their lower refractive index and corresponding weaker confinement, it was not obvious whether the same dispersion engineering techniques previously explored in silicon can be used, and whether similar low losses can be achieved. To investigate these issues, we have fabricated dispersion engineered chalcogenide photonic crystal waveguides and demonstrated losses as low as 21dB/cm. In addition, we have shown that the dispersion engineering toolkit can be applied to the chalcogenide system and have demonstrated slow light waveguides with a group index of $n_g \approx 40$. Given the lower phase index n_φ of the waveguide mode, this corresponds to a slowdown factor ($S = n_g/n_\varphi$) of $S \approx 20$, which is considerable and highlights the potential of the system for nonlinear applications. To our knowledge, this is the first demonstration of systematic dispersion engineering in relatively low refractive index photonic crystal waveguides, in particular in chalcogenides. Furthermore, we have shown the benefits of using vapour phase HF etching for the fabrication of photonic crystal membranes.

Acknowledgements

The authors would like to thank T. P. White for the helpful discussions on dispersion engineering. Marcel Spurny was supported by the EU FP6 program SPLASH. Support of the Australian Research Council through its Centre of Excellence Program is gratefully acknowledged.

#137250 - $15.00 USD Received 3 Dec 2010; revised 13 Jan 2011; accepted 13 Jan 2011; published 19 Jan 2011